

DOI: 10.24425/amm.2021.136421

 BYUNGJOO CHOI<sup>1†</sup>, YONGJUN CHOI<sup>1†</sup>, MOON GU LEE<sup>1</sup>,  
 JUNG SUB KIM<sup>2</sup>, SANG WON LEE<sup>2</sup>, YONGHO JEON<sup>1\*</sup>

## DEFECT DETECTION USING DEEP LEARNING-BASED YOLOV3 IN CROSS-SECTIONAL IMAGE OF ADDITIVE MANUFACTURING

Deposition defects like porosity, crack and lack of fusion in additive manufacturing process is a major obstacle to commercialization of the process. Thus, metallurgical microscopy analysis has been mainly conducted to optimize process conditions by detecting and investigating the defects. However, these defect detection methods indicate a deviation from the operator's experience. In this study, artificial intelligence based YOLOv3 of object detection algorithm was applied to avoid the human dependency. The algorithm aims to automatically find and label the defects. To enable the aim, 80 training images and 20 verification images were prepared, and they were amplified into 640 training images and 160 verification images using augmentation algorithm of rotation, movement and scale down, randomly. To evaluate the performance of the algorithm, total loss was derived as the sum of localization loss, confidence loss, and classification loss. In the training process, the total loss was 8.672 for the initial 100 sample images. However, the total loss was reduced to 5.841 after training with additional 800 images. For the verification of the proposed method, new defect images were input and then the mean Average Precision (mAP) in terms of precision and recall was 0.3795. Therefore, the detection performance with high accuracy can be applied to industry for avoiding human errors.

*Keywords:* Additive manufacturing, Deposition defect, Data augmentation, YOLOv3, Object detection

### 1. Introduction

Additive manufacturing (AM) is drawing attention as a key part of the fourth industrial revolution, presenting a new paradigm in production technology. Unlike conventional subtractive manufacturing, materials are laminated in line by line and layer upon layer, and by the topology optimization it produces not only complex shapes but also excellent rigid parts. AM can also help rapid production and automation, as well as reduce resource efficiency and weight. However, to apply AM parts to structures subject to high loads such as aircraft or automobiles, a process is needed to ensure integrity of internal defects. Thus, the metallurgical microscopy analysis has been primarily conducted to optimize process conditions in to detect and investigate the defects. However, these defect detection methods show variations by the operator's experience.

Many studies have been conducted to reduce anomalies and automatically overcome the limitations of product integrity by applying deep learning to AM [1-8].

Kwon et al. [1] used the Artificial Neural Network (ANN) to find the porosity and crack in real-time Selective Laser Melting (SLM) process. The light emitted from the melting pool was understood that microstructures of the part were influenced by the laser power. Therefore, the intensity was measured as the number of pixels with using a high-speed camera and used for input data of algorithm training. Consequently, defects were precisely classified through real-time melting pool monitoring.

Scime et al. [2-5] researched the Laser-Powder Bed Fusion (L-PBF) process in terms of melt pool monitoring and anomaly classification with using the high-speed camera and machine learning algorithm. The Multi Scale Convolutional Neural Network (MsCNN), Back of Words (BoW), and Convolutional Neural Network (CNN) algorithms were trained using the experimental image data. Anomalies were more accurately classified by the MsCNN algorithm which can enlarge the defect area than others.

Khanzadeh et al. [6-8] detected the anomaly signatures from the AM process monitoring. Especially, a real-time porosity

<sup>1</sup> AJOU UNIVERSITY, DEPARTMENT OF MECHANICAL ENGINEERING, 206, WORLD CUP-RO, YEONGTONG-GU, SUWON-SI, GYEONGGI 16499, REPUBLIC OF KOREA

<sup>2</sup> SUNGKYUNKWAN UNIVERSITY SCHOOL OF MECHANICAL ENGINEERING, SUWON, REPUBLIC OF KOREA

\* Corresponding author: princaps@ajou.ac.kr

† These Authors Contributed Equally to this Work



prediction method was developed using morphological characteristics and thermal images of the melt pool. Six algorithms were compared from two perspectives. K-Nearest Neighbor (KNN) showed a highest accuracy classification performance of 98.44%. And Decision Tree (DT) had a 0.03% lower probability of mistaking the normal melt pool as pores. Supervised learning combined with morphological models showed about 250% better performance in predicting abnormal molten pool than general supervised learning.

Previous studies have focused on the study of CNN-based classification algorithms to find the label of defects in multi classes. On the other hand, real-time object detection algorithms in self-driving cars have been attracting much attention, lately. Therefore, a study was conducted to detect metal defects using YOLOv3 [9], a kind of object detection algorithm. A code capable of fast and high-accuracy object detection with only 9 lines was used from ImageAI [10] of the Python library. In preparation, training data was created by adding annotations of bounding boxes and labels to defect images, and the number of data was augmented to maximize the effect of learning. After data setup, the training progress of the YOLOv3 was evaluated as the total loss. And the detection evaluation was performed as the mean Average Precision (mAP) from the point of view of precision and recall. Finally, ability was confirmed whether the trained YOLOv3 can accurately find and label defects by inputting new images.

## 2. Data preparation

While classification algorithms train the division of the image itself, object detection is a method of training the recognition of specific objects within the image. Therefore, the training data of object detection should provide annotation information including the coordinates and classes along with the images. This chapter describes the process of preparing training data of defects occurring in the metal AM process. Firstly, 100 images which have defects such as porosity, crack, and lack of fusion of alone or multiple or complex form were prepared from web crawling. Due to the characteristic of pixel-by-pixel training, images were cropped to 500×500 pixels to reduce the training time and hardware resource usage. And annotations were added to the entire image using the graphical image tool [11] as shown in Fig. 1(a). Because the annotation process determines the detection performance of the algorithm, a cross-sectional analysis expert was needed to accurately perform bounding box and labeling for defects. The training data was made as a pair of image file and annotation file of Pascal VOC form from the ImageNet [12].

To train an object detection algorithm based on image, a large number of data is required. For this, an image augmentation that creates a new image by slightly transforming (i.e. translation, rotation, resize, cropping, padding, etc.) the original image from imgaug [13] of the Python library was applied. Prior to augmentation, reduced the image and black padding was added

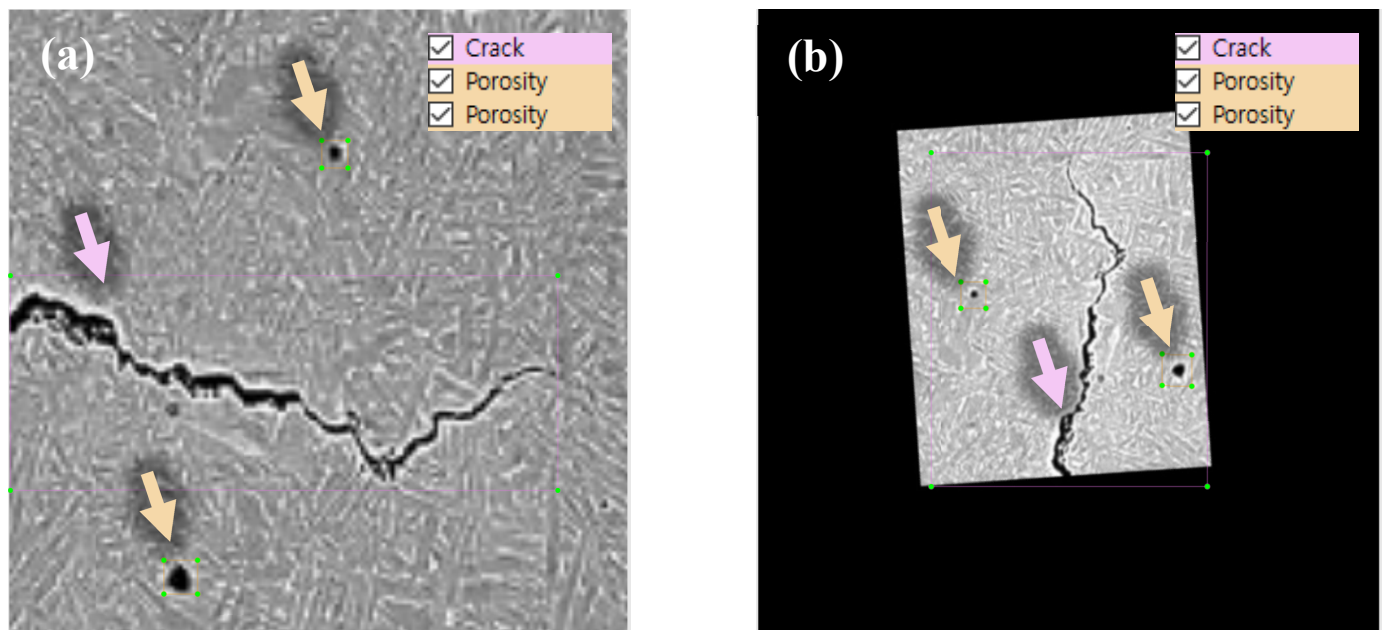


Fig. 1. Training image for defect detection with annotations: (a) Raw data, (b) After data augmentation

TABLE 1

The number of data set and training information

	Training data	Validation data	Epoch	Computing time (h)	Class		
					Porosity	Crack	Lack of fusion
Raw image	80	20	50	22	159	96	36
After augmentation	640	160	20	96	1272	760	288

to prevent training errors due to the protrusion of the bounding box. Consequently, 80 training images and 20 validation images were amplified to 640 training images and 160 validation images, as shown in Fig. 1(b) and Table 1.

### 3. Training and validation

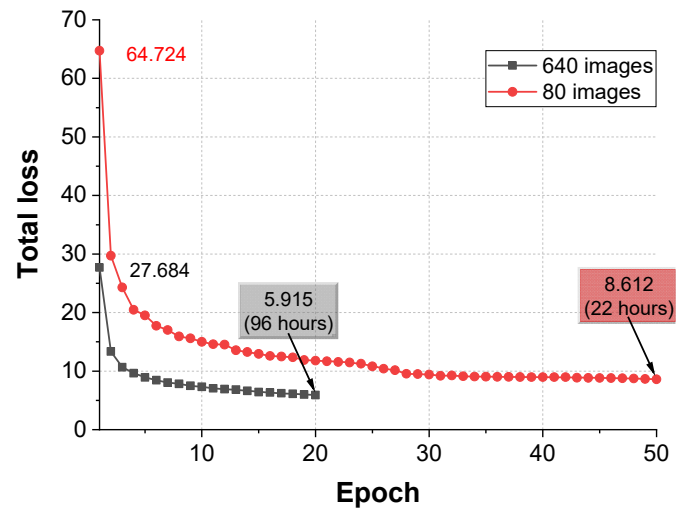
Other object detection algorithms improve computational efficiency by applying selective search or region proposal network (RPN) based on the sliding window method for finding objects. While YOLOv3 divides the entire image into relatively large cell grid and detects objects at once, enabling very fast computing. Thus the total loss representing the training progress calculate the sum of the localization loss for location accuracy, the confidence loss of the existence in the cell, and the classification loss of the classification accuracy of the objects.

In this study, pre-trained YOLOv3 was used as a feature extractor to improve learning efficiency, and classifier was trained with the custom data (from Ch. 2). The computing was performed using i7-6700K 4.00GHz (Intel) CPU and GeForce GTX 1050Ti (NVIDIA) graphic card. The progress of the total loss in the training process is shown in Fig. 2(a). The training starts with a relatively low loss in 640 images, because 1 epoch of many images determines the weight and bias with a large amount of learning than less images. 640 images went down to a total loss of 8.460(6 epochs, 28.8 hours) which was lower than 8.612(50 epochs, 22 hours) of the training finish of small amount of images. Consequently, the learning of many images by the augmentation was reduced to a total loss of 5.915 in 96 hours, confirming relatively excellent detection performance.

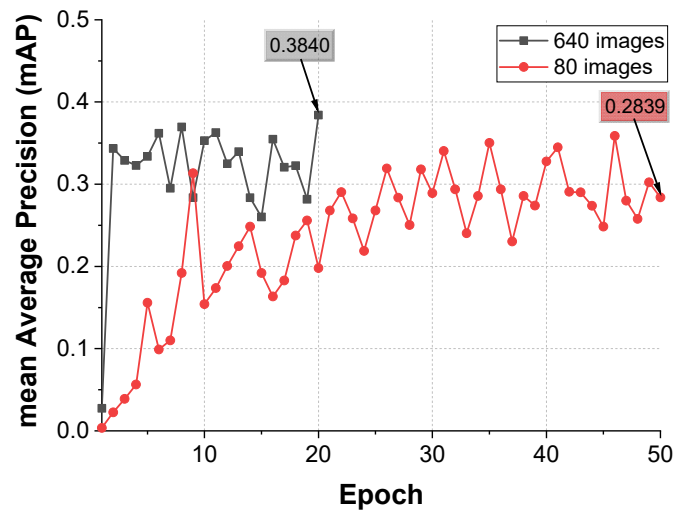
The validation of the trained model was performed according to the epoch. First, the average precision (AP) for each class of porosity, crack, and lack of fusion was derived for each epoch, and the average AP for each class was mAP. AP is the area of the curve for two things: recall (x-axis), which evaluates the number of objects found among the ground truth and precision(y-axis), which evaluate the number of ground truth among the number of objects found. And the intersection over union (IoU) representing the overlap between the ground truth box and the prediction box was set to 0.5. Therefore, the derived mAP graph is shown in Fig. 2(b). In the last epoch, AP of 640 images were 0.3840 and higher than 0.2839 in the training of 80 images. In a different way, the detection performance was evaluated using a higher mAP model before the last epoch, but it had poor performance because the low total loss. In order to reduce eccentric training and obtain a stable mAP, further research was needed by increasing the epochs.

### 4. Defect detection test

The performance of defect detection is determined by how accurate results are output when a new image is input to the trained model. So, the output result according to the amount



(a) Training progress by Total loss

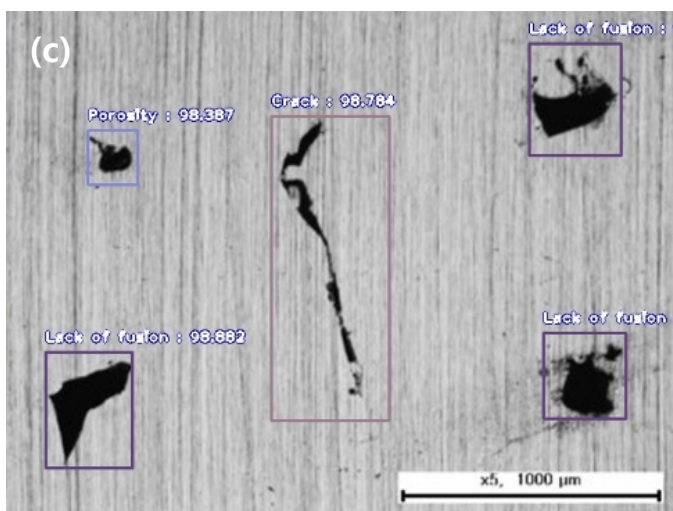
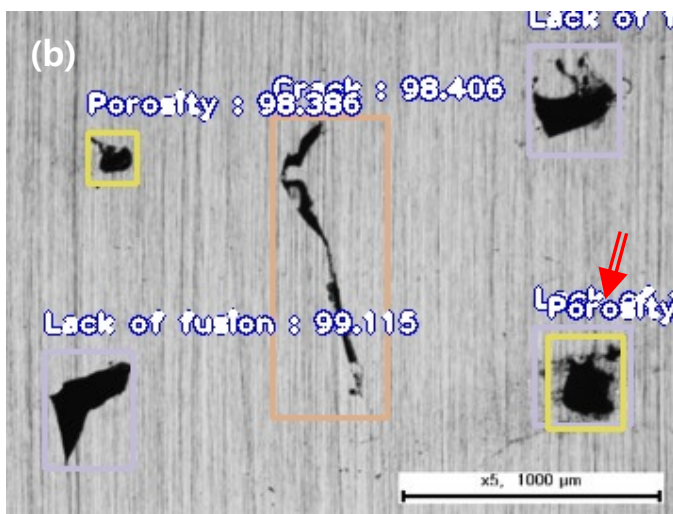
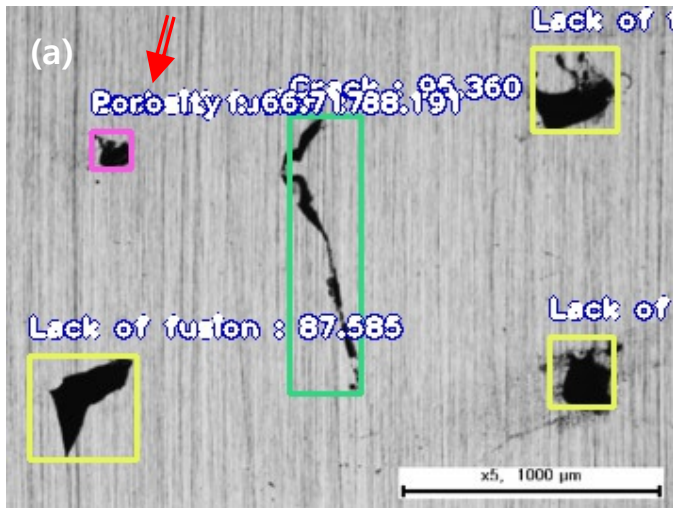


(b) Validation progress by mAP

Fig. 2. Training and validation process: (a) Training progress by Total loss, (b) Validation progress by mAP

of training data and the input image pixel size was studied by inputting a complex defect image as shown in Fig. 3. The higher detection confidence for each defect was confirmed in Fig. 3(b) when the number of training data was large. However, regardless of the amount of training data, the superposition error (Red arrow) is shown in Fig. 3(a) and (b). This problem was solved by increasing the number of pixel data for defect analysis from the extending the resolution of the input image (Fig. 3(c)). Alternatively, object with low confidence can be removed by adjusting the factor of minimum percentage probability or non-maximal suppression threshold. In particular, this test showed the detection performance of not misrecognizing the longitudinal hairline existing by polishing as a crack. And the defect detection took 14 seconds regardless of the image size and amount of training each Fig. 3(a), (b), (c).

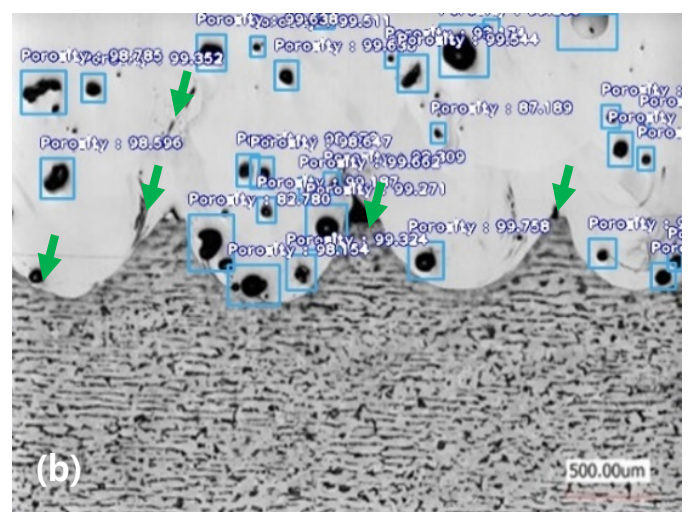
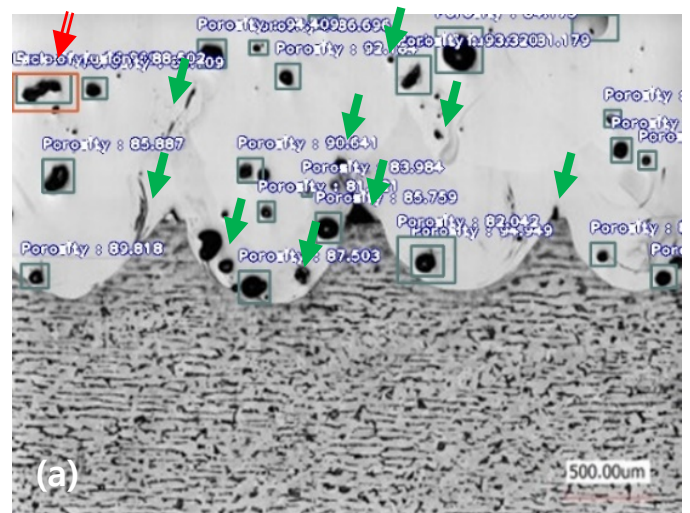
The detection performance was evaluated in more defected image as shown in Fig. 4. Obviously, a number of undetected



\*Red arrow (  $\leftrightarrow$  ): superposition error

Fig. 3. Defect detection test according to the amount of training: (a) 80 images training model (355×267 pixel), (b) 640 images training model (355×267 pixel), (c) 640 images training model (688×500 pixel)

errors (Green arrow) and also superposition error (Red arrow) were more found in high total loss and low mAP model as shown in Fig. 4(a). On the other hand, the model after training



\*Red arrow (  $\leftrightarrow$  ): superposition error

\*Green arrow (  $\leftarrow$  ): undetected error

Fig. 4. Defect detection test according to the training epochs (640 images training and 688×500 pixel) [14]: (a) 2 epochs in 9 hours (total loss = 13.361, mAP = 0.3433), (b) 20 epochs in 96 hours (total loss = 5.915, mAP = 0.3840)

to 20 epochs succeeded in detecting most defect (Fig. 4(b)). Nevertheless, undetected errors were confirmed, and in particular, it showed a vulnerability to the detection of crack and lack of fusion. The trained YOLOv3 has tendency to be partial in detecting caused by training of more than 1.6 times of the porosity class (Table 1) [15]. It is necessary to derive improved results by preparing learning data that included unbiased class in the next study. The excellent performance of not erroneously detecting the material phase of the base material as crack and porosity was confirmed. The defect detection took 14 seconds regardless of the amount of training each Fig. 4(a), (b). Comprehensively, since defects can be precisely detected at a fast inspection speed and coordinates in pixel units can be output, automated post-processing such as precise measurement or defect recovery are possible.

## 5. Conclusions

In this study, latest object detection algorithm of the YOLOv3 model was evaluated whether AM defects can be detected. 100 data sets were prepared by inputting the bounding box and label to the defect of the training data, and amplified into 640 pair of training data and 160 pair of validation data by the augmentation algorithm. The data sets were trained by 20 epochs for 96 hours, resulting in a total loss of 5.915 and a mAP of 0.2839 in validation step of 160 data sets. As a result, the greater the training amount, epochs, and the size of the analyzed image, the more accurate defect detection performance was confirmed. However, due to the defect class biased in porosity, the detection performance of lack of fusion and crack was relatively degraded. Nevertheless, automated post-processing is possible because the pixel-unit coordinates of the defect were derived. Consequently, the defect detection took constantly 14 seconds regardless of the image size and amount of training. In future research, we will prepare a lot of training data considering unbiased class in order to secure better detection performance. And the sufficient hardware or cloud computing service will be used to learn more epochs. Therefore, the result of this study are expected to apply object detection algorithm to industry for avoiding human errors.

## Acknowledgments

This work was supported by the Korea Institute of Energy Technology Evaluation and Planning (KETEP) and the Ministry of Trade, Industry & Energy (MOTIE) of the Republic of Korea (No. 20206410100080).

## REFERENCES

- [1] O.H. Kwon, H.G. Kim, M.J. Ham, W.R. Kim, G.H. Kim, J.H. Cho, N.I. Kim, K.I. Kim, *J. Intel. Manuf.* **31**, 375-386 (2020).
- [2] L. Scime, J. Beuth, *Addit. Manuf.* **24**, 273-286 (2018).
- [3] L. Scime, J. Beuth, *Addit. Manuf.* **19**, 114-126 (2018).
- [4] L. Scime, J. Beuth, *Addit. Manuf.* **25**, 151-165 (2019).
- [5] L. Scime, J. Beuth, *Addit. Manuf.* **29**, 100830, 1-9 (2019).
- [6] M. Khanzadeh, W. Tian, A. Yadollahi, H.R. Doude, M.A. Tschopp, *Addit. Manuf.* **23**, 443-456 (2018).
- [7] M. Khanzadeh, S. Chowdhury, M. Marufuzzaman, M.A. Tschopp, L. Bian, *J. Manuf. Syst.* **47**, 69-82 (2018).
- [8] M. Khanzadeh, S. Chowdhury, M.A. Tschopp, H.R. Doude, M. Marufuzzaman, L. Bian, *IISE Trans.* **51**, 5, 437-455 (2019)
- [9] J. Redmon, A. Farhadi, arXiv preprint, 1804.02767 (2018).
- [10] <https://imageai.readthedocs.io/en/latest/>
- [11] <https://github.com/tzutalin/labelImg>
- [12] <http://www.image-net.org/>
- [13] <https://imgaug.readthedocs.io/en/latest/index.html>
- [14] J.S. Kim, B.J. Kang, S.W. Lee, *J. Mech. Sci. Technol.* **33**, 12, 1-7 (2019).
- [15] A. Torralba, A.A. Efros, *Proc. CVPR IEEE* 12218709, 1521-1528 (2011).